Title: Evidence for immediate enhancement of medial-temporal lobe memory processing by network-targeted theta-burst stimulation during concurrent fMRI

Abbreviated title: Immediate theta-burst impact on memory

Authors: Molly S. Hermiller*[1-4], Yu Fen Chen[5], Todd B. Parrish[1,5,6], and Joel L. Voss[1-4]

Affiliations:

[1] Interdepartmental Neuroscience Program, Northwestern University
[2] Department of Medical Social Sciences, Feinberg School of Medicine, Northwestern University
[3] Ken & Ruth Davee Department of Neurology, Feinberg School of Medicine, Northwestern University
[4] Department of Psychiatry and Behavioral Sciences, Feinberg School of Medicine, Northwestern University
[5] Department of Radiology, Feinberg School of Medicine, Northwestern University
[6] Department of Biomedical Engineering, McCormick School of Engineering and Applied Science, Northwestern University

***Correspondence t**o: molly.hermiller@northwestern.edu

Conflict of interest: The authors declare no competing financial interests.

Acknowledgments: We thank Rachael A. Young and Stephen VanHaerents for contributing to data collection. Neuroimaging was performed at the Northwestern University Center for Translational Imaging, supported by Northwestern University Department of Radiology. This research was supported in part through the computational resources and staff contributions provided for Quest, the high-performance computing facility at Northwestern University, which is jointly supported by the Office of the Provost, the Office for Research, and Northwestern University Information Technology. This research was supported by R01-MH106512 and R01-MH111790 from the National Institute of Mental Health and by T32-NS047987 and F31-NS111892 from the National Institute of Neurological Disorders and Stroke. The content is solely the responsibility of the authors and does not necessarily represent the official view of the National Institutes of Health.

Abstract: The hippocampus supports episodic memory via interaction with a distributed brain network. Previous experiments using network-targeted noninvasive brain stimulation have identified episodic memory enhancements and modulation of activity within the hippocampal network. However, mechanistic insights were limited because these effects were measured long after stimulation and therefore could have reflected various neuroplastic aftereffects with extended timecourses. In this experiment with human subjects of both sexes, we tested for immediate stimulation impact on memory-related activity of the hippocampus and surrounding cortex of the medial-temporal lobe (MTL) by delivering theta-burst transcranial magnetic stimulation (TBS) concurrent with fMRI, as an immediate impact of stimulation would suggest an influence on neural activity. We reasoned that TBS would be particularly effective for influencing the MTL because rhythmic neural activity in the theta band is associated with MTL memory processing. First, we demonstrated that it is possible to obtain robust fMRI signals of MTL activity during concurrent TBS. We then identified immediate effects of TBS on memory encoding of visual scenes. Brief volleys of TBS targeting the hippocampal network increased MTL activity during scene encoding and strengthened subsequent recollection. Stimulation did not influence MTL activity during an interleaved numerical task with no memory demand. Control conditions using beta-band stimulation and out-of-network stimulation also did not influence MTL activity or memory. These findings indicate that TBS targeting the hippocampal network immediately impacts MTL memory processing. This suggests direct, beneficial influence of stimulation on MTL neural activity related to memory and supports the role of theta-band activity in human episodic memory.

Significance Statement: Theta-burst noninvasive stimulation targeting the human hippocampal network immediately impacted memory processing measured during concurrent fMRI, suggesting that this rhythm is relatively privileged in its ability to influence neural activity related to memory.

Introduction

The hippocampus exhibits theta-band (~4-8 Hz) oscillatory neural activity that is thought to provide a temporal framework for coding information about life experiences into enduring memories (Buzsaki, 2002; Lisman and Jensen, 2013; Herweg et al., 2020). This memory function involves hippocampal interaction with a network of interconnected brain regions in medial-temporal, parietal, and prefrontal cortex (Squire and Zola-Morgan, 1991; Squire et al., 2004; Eichenbaum et al., 2007; Battaglia et al., 2011; Ranganath and Ritchey, 2012) which show interregional synchrony of memory-related activity preferentially in the theta band (Fell et al., 2001; Buzsaki and Draguhn, 2004; Foster et al., 2013; Lisman and Jensen, 2013; Staudigl and Hanslmayr, 2013). Although the functional significance of hippocampal theta oscillatory activity has been experimentally tested via stimulation in rodents (Shirvalkar et al., 2010; Zutshi et al., 2018), such direct functional tests present major challenges for human experimentation. It is reasonable to think that electrical stimulation of the hippocampus using a theta-rhythmic pattern, as in theta-burst stimulation (TBS; volleys of high-frequency stimulation delivered in a theta rhythm), should be capable of testing the role of theta in episodic memory. This is because theta-rhythmic stimulation such as TBS mimics the endogenous theta rhythm thought to support hippocampal memory processing and hippocampal network synchronization, and therefore should optimally influence this network's function via activity entrainment (Thut et al., 2011b; Chanes et al., 2013; Romei et al., 2016; Thut et al., 2017). However, direct electrical stimulation of the hippocampus and its immediate entorhinal inputs via depth electrodes in human neurosurgical cases typically disrupts memory, without necessary specificity to the theta band (Coleshill et al., 2004; Jacobs et al., 2016; Goyal et al., 2018).

An alternative approach targets the hippocampus indirectly via stimulation of its network. For instance, invasive electrical stimulation of the lateral temporal cortex area of the hippocampal network enhanced verbal memory in four human neurosurgical cases (Kucewicz et al., 2018) and "closed-loop" stimulation of approximately the same location based on neural correlates of successful memory caused a relative enhancement compared to the same stimulation of other brain regions, which was disruptive (Ezzyat et al., 2018). Of relevance to the theta rhythm, memory enhancement was achieved in a pilot study of four cases receiving TBS of the fornix (Miller et al., 2015). Further, TBS with microstimulation of

entorhinal cortex enhanced memory in several cases in which white matter (rather than gray matter) was targeted, presumably due to greater effects on network synchrony due to white matter stimulation (Titiz et al., 2017). These studies have provided preliminary evidence that invasive stimulation of the hippocampal network might modulate episodic memory, including when stimulation is delivered in a theta-rhythmic pattern. However, demonstrations of memory enhancement by invasive TBS (Miller et al., 2015; Titiz et al., 2017) did not include non-theta control stimulation frequencies, and therefore do not permit strong conclusions regarding the specific role of theta rhythms in human memory.

Noninvasive stimulation can also be used to test putative network functional properties (Fox et al., 2012). Robust group-level enhancement of episodic memory has been reported in multiple studies targeting the hippocampal network using noninvasive transcranial magnetic stimulation (TMS) in healthy individuals (Hebscher and Voss, in press). Network-targeted TMS increased hippocampal network fMRI connectivity and memory-related fMRI activity, and improved memory performance for hours to weeks after stimulation delivery (Wang et al., 2014; Kim et al., 2018; Tambini et al., 2018; Freedberg et al., 2019; Hermiller et al., 2019; Warren et al., 2020). One study using network-targeted TMS found that TBS had greater impact on memory accuracy and memory-related hippocampal fMRI connectivity than did TMS using a non-theta (20-Hz) control frequency (Hermiller et al., 2018). This finding is consistent with the hypothesized importance of hippocampal network theta activity for memory. However, a weakness of previous noninvasive stimulation experiments with respect to mechanistic interpretation is that these studies measured long-lasting aftereffects of stimulation (ranging from minutes to weeks), which could be mediated by a variety of indirect neuroplasticity mechanisms (Thickbroom, 2007). Better evidence for preferred influence of TBS on memory-related neural activity would require immediate assessment of stimulation impact.

To address this issue, we delivered TBS to a hippocampal-network-targeted location in the parietal cortex during concurrent fMRI while subjects performed a memory task. We developed custom fMRI parameters that allowed TBS as well as control-frequency (12.5 Hz) stimulation during concurrent fMRI without stimulation-related imaging artefact in areas of interest. Due to the neuroimaging limitations of concurrent TMS-fMRI, such as lack of full-brain coverage and signal distortion near the TMS coil, we

103 focused on effects of TBS on hippocampus and adjacent cortex of the medial temporal lobe (MTL), as
104 high-quality fMRI signals could be obtained from these areas using our procedure.
105 Human subjects studied complex visual scenes that were each immediately preceded by different
106 stimulation conditions. We hypothesized that TBS in the seconds immediately preceding individual scene
107 stimuli would improve encoding success and increase fMRI signals of successful encoding in the MTL.
108 The premise of this prediction is that greater MTL theta activity predicts more successful memory
109 formation, particularly for complex associative memory information (Rutishauser et al., 2010; Fell et al.,
110 2011; Herweg et al., 2020), and that TBS may increase the theta rhythm in the MTL due to neural
111 entrainment (Thut et al., 2011a; Hanslmayr et al., 2019). We further hypothesized that enhancement of
112 memory encoding and fMRI activity by TBS targeting the hippocampal network would be selective versus
113 various control conditions, including controls for the cognitive task (memory versus non-memory), for the
114 stimulation rhythm (theta versus non-theta), for the stimulation target (hippocampal-network-targeted
115 versus out-of-network location), and for the hemisphere in which the hippocampal network was targeted
116 (left versus right). Immediate and selective effects of hippocampal-network-targeted TBS on MTL
117 memory-related activity would suggest that noninvasive stimulation can impact targeted regions' neural
118 activity, rather than longer-term neuroplasticity processes, and would support the role of theta in human
119 memory formation.
120
121 **Materials and Methods**
122 Overview
123 Following a baseline session, subjects completed a two-day experiment in which they attempted to
124 remember complex visual scenes that were each immediately preceded by different stimulation
125 conditions, performed during fMRI scanning. The main condition of interest was TBS delivered to a
126 hippocampal-network targeted (HNT) location in the parietal cortex immediately before the onset of
127 scenes. Several control conditions were used to test specificity. Subjects also received stimulation
128 immediately before the presentation of numeric judgments, interleaved randomly with the scenes
129 throughout the task (Fig. 1A). We expected no effect of stimulation on hippocampal activity for this
130 condition, as hippocampal activity is generally not evoked by numeric judgments (Stark and Squire,

2001) and therefore would not increase via direct effects of stimulation on hippocampal neural activity. Furthermore, the same scene and number conditions were administered in three control stimulation conditions: (i) a different stimulation pattern (beta; 12.5 Hz) (Fig. 1B) applied to the same HNT location, (ii) TBS applied to a control location in the supplementary motor area (SMA) outside the hippocampal network (Fig. 1C), and (iii) beta stimulation of the SMA location. None of these control conditions were expected to influence downstream MTL activity. Finally, stimulation was not delivered for a subset of scene and number trials, providing a no-stimulation ("off") control condition. Scene and number trials with and without stimulation were intermixed throughout scanning sessions, guarding against confounding influences such as stimulation-induced fMRI artifact and stimulation carry-over effects across trials. All conditions were administered in each subject using a within-subjects counterbalanced design over two experimental sessions (Fig. 1D).

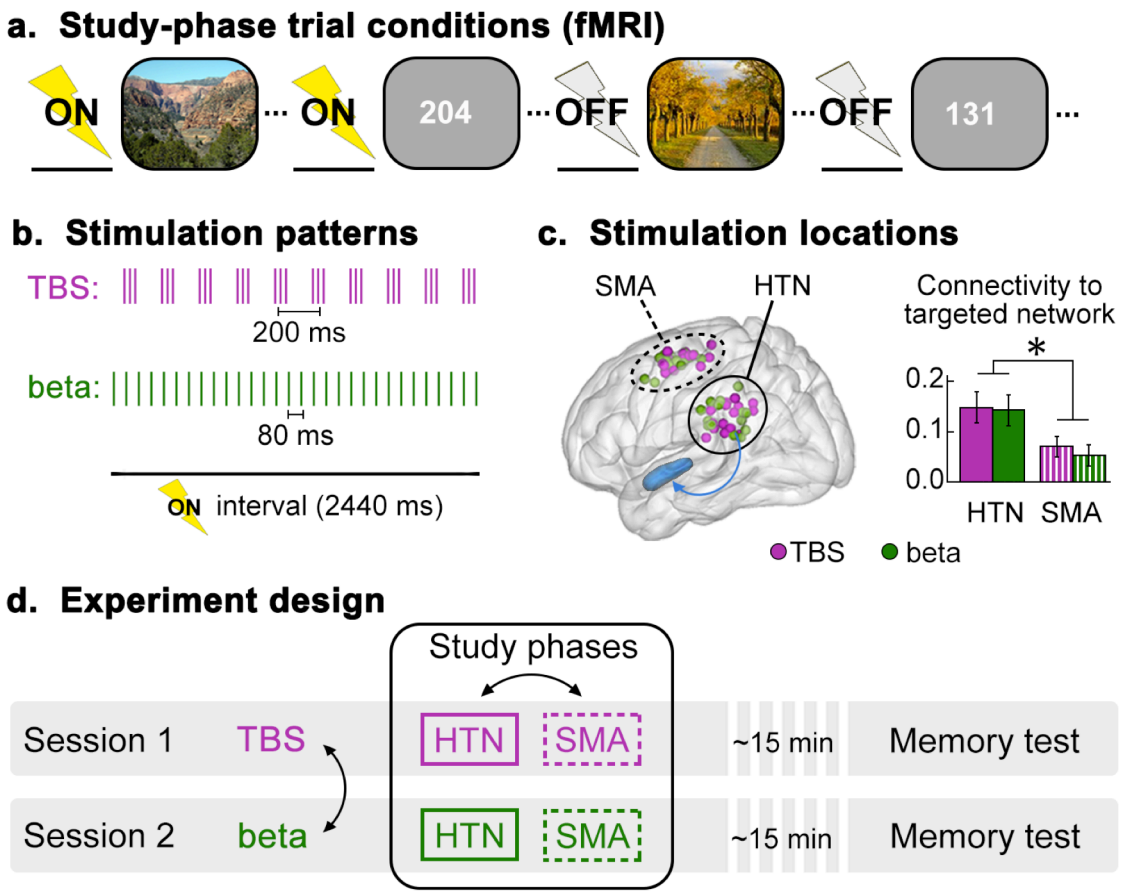

Figure 1. Trial-specific stimulation during episodic memory formation. (A) Scene-encoding and numeric-judgment trials were randomly intermixed during each study phase, with ~2 s of stimulation delivered immediately before stimulus onset for a subset of trials (ON) and no preceding stimulation for remaining trials (OFF). Study phases were completed during fMRI scanning with memory test phases after scanning. There were four stimulation conditions for ON and OFF trials. (B) Stimulation was delivered as either a theta-burst pattern (TBS: 50 Hz triplet pulses delivered at 5 Hz) or at beta (single pulses delivered at 12.5 Hz). These conditions had the same overall number of pulses during each stimulation period delivered at the same intensity. (C) Stimulation was delivered to the HNT parietal location (based on its fMRI connectivity with left hippocampus, as depicted by the blue arrow), or a control out-of-network SMA location. Achieved stimulation locations confirmed via MRI for each condition and subject are indicated by colorized spheres on a template brain. Bar plots represent mean ±s.e.m. baseline resting-state fMRI connectivity of the subject-specific stimulation locations with the hippocampal network, confirming relatively higher connectivity for the HNT than SMA location. *P<0.05 main effect of location by one-way rmANOVA. (D) HNT or SMA locations were targeted for one of the two study phases in each experimental session. After both study phases were complete, subjects exited the scanner for a ~15 min break before taking the memory test. A different stimulation pattern (TBS or beta) was used for each experimental session. Black arrows indicate stimulation conditions with order counterbalanced across subjects.

143 Subjects

144 Adult subjects passed standard MRI and TMS safety screenings (Rossi et al., 2009), reported no present
145 use of psychoactive drugs, and were free of known neurological and psychiatric conditions. Datasets
146 from 16 subjects were included in all reported analyses (8 females, ages 20-35 years, average
147 age=27.6, SD=4.32). Data from two additional subjects were collected but excluded from all reported
148 analyses due to poor behavioral performance (overall miss rate > 50%). In addition, data collection was
149 attempted from three additional subjects but failed due to technical malfunction (n=2) or attrition (n=1).
150 Subjects gave written informed consent approved by the Northwestern University Institutional Review
151 Board and were paid for participation. The sample size of N=16 was chosen to match or exceed previous
152 experiments that demonstrated memory improvement for stimuli encoded following short volleys of TMS
153 (i.e., <2 s TMS immediately before stimulus onset) (Kohler et al., 2004; Demeter et al., 2016).

154

155 Baseline session

156 Subjects completed a baseline session to determine stimulation locations and intensity prior to two
157 experimental sessions, performed on different days (described below).

158

159 *Baseline MRI to determine stimulation locations*

160 Resting-state fMRI and structural MRI were collected using a 3T Siemens PRISMA scanner with
161 a 64-channel head/neck coil. Baseline resting-state functional images were acquired using a blood-
162 oxygenation-level-dependent (BOLD) contrast sensitive gradient-echo echo-planar imaging (EPI)
163 pulse sequence (270 frames; TE 20 ms; TR 2000.0 ms; flip angle 80°; voxel resolution 1.7 mm isotropic;
164 70 ascending axial slices; 210x203 mm FOV; scan duration 9 min). During the resting-state scan
165 subjects were instructed to lie as still as possible, to keep their eyes open and focused on a fixation cross
166 presented in the center of the screen, and to let their minds wander. Structural images were acquired
167 using a T1-weighted MPRAGE sequence (176 frames; TE 1.69 ms; TR 2170 ms; TI 1100 ms; flip angle
168 7°; voxel resolution 1.0 mm isotropic; 256x256 mm FOV; GRAPPA acceleration of a factor of 2; scan
169 duration 6.36 min).

Baseline scans were submitted to resting-state fMRI connectivity analysis to determine stimulation locations. All fMRI analyses used AFNI (Cox, 1996) and were visualized with the BrainNet Viewer Matlab (The MathWorks, Inc. Natick, MA, USA) toolbox (Xia et al., 2013) on a smoothed Colin27 template. Anatomical scans were skull-stripped (*3dSkullStrip*) and co-registered to standardized space using the Colin27 template (*auto_tlrc*). Preprocessing of the functional volumes included outlier suppression (*3dDespike*), slice timing and motion correction (*3dvolreg*), and co-registration to the anatomical scan (*align_epi_anat*). The transformations were applied simultaneously in a single resampling step (*3dAllineate*). Motion parameters were calculated for each volume as the Euclidean norm of the first difference of six motion estimates (three translation and three rotation). Volumes with excessive motion (>0.2 mm), as well as the previous volume, were censored. On average, 0.42% (SD=1.11, range=0-4.44%) of the resting-state volumes were censored. Data were spatially smoothed using a 4-mm full-width-at-half-maximum (FWHM) isotropic Gaussian kernel (*3dmerge*) and signal intensity was normalized by the mean of each voxel. EPI masks were created that included only voxels in the brain that were not excluded due to instability by *3dAutomask*. Bandpass filtering (0.01-0.1 Hz), motion censoring, and nuisance time series (estimates of motion parameters and their derivatives) were detrended from each voxel simultaneously (*3dDeconvolve, 3dTproject*) to yield a residual time series used in connectivity analyses.

Seed-based resting-state fMRI connectivity was used to determine subject-specific stimulation locations used in the subsequent concurrent TMS-fMRI experimental sessions. For each subject, a 2 mm seed in the left hippocampus (MNI: -30 -18 -18) was used in a seed-based functional connectivity analysis (*3dTcorr1D*) to identify a left lateral parietal cortex location with robust fMRI connectivity to a left hippocampal seed (mean z(r)=0.38, SD=0.05; average MNI: -53 -41 27). This was the stimulation location used for hippocampal-network-targeted (HNT) stimulation (Fig. 1C). The control out-of-network stimulation location was set in the left supplementary motor area (SMA; average MNI: -36 -3 67), a region outside of the targeted hippocampal network. Both the HNT and SMA locations allowed the TMS coil to be positioned in the scanner without blocking the subjects' view of the screen. Due to coil displacement during scanning, the actual achieved stimulation locations deviated from these intended targets (see below and Fig. 1C).

198

199 *Stimulation intensity determination*

200 TMS was delivered with a MagPro X100 stimulator using a MagPro MRi-B91 air-cooled butterfly
201 coil and MRI-compatible TMS setup (MagVenture A/S, Farum, Denmark). Resting motor threshold (RMT)
202 was found during the baseline session in order to determine the stimulation intensity used during the
203 experimental sessions (see below). Subjects sat at the entrance of the MRI bore with their arms resting
204 comfortably during RMT determination. The MRi-B91 TMS coil was used to determine RMT as the
205 minimum percentage of stimulator output (% SO) necessary to generate a visible contraction of the right
206 thumb (*abductor pollicis brevis)* for five out of ten consecutive single pulses. Pulses were biphasic, as
207 were pulses delivered during experimental sessions. RMT values ranged between 45.0-85.0% SO
208 (mean=61.6, SD=10.8).

209

210 <u>Experimental Sessions</u>

211 Following the baseline session, subjects returned for two experimental TMS/fMRI sessions on separate
212 days to complete a 2x2 crossover design. One stimulation pattern (TBS or beta) was used during each
213 session. Within each session, there were two study phases that differed in stimulation location (HNT or
214 SMA). The order of these conditions (TBS or beta session; HNT-then-SMA or SMA-then-HNT within
215 each session) was counterbalanced across subjects. Memory for scenes encoded during both study
216 phases was tested at the end of the experimental session, after subjects finished MRI scanning.

217

218 *Experiment Design*

219 There were two study phases during each of the two experimental sessions. Each study phase
220 lasted ~70 min and comprised 144 trials (288 trials total for the session). Each trial began with a white
221 fixation cross presented in the center of the screen, during which ~ 2 s stimulation was delivered (see
222 TMS/fMRI acquisition methods for exact timing). Immediately following stimulation, a visual stimulus was
223 presented for 2 s. The study item was followed by a white fixation cross that remained on the screen until
224 the next trial for a randomly varied duration between 11-19.5 s. Different visual stimuli were presented
225 during each study phase. Complex visual scenes (50% of trials; 144 scenes total for the session) were

226 randomly intermixed with numeric stimuli (50% of trials; 144 numbers total for the session). During the
227 scene presentation, subjects were instructed to imagine visiting the depicted location and to rate via
228 button press whether they would like to visit the location (right hand button) or not (left hand button).
229 Scenes were chosen from the SUN397 dataset (Xiao et al., 2016) based on the following criteria:
230 complex outdoor natural scenes (e.g., mountains, beaches, forests, waterfalls, deserts) without
231 prominent humans, animals, or man-made objects; color image; image did not include text. Subjects
232 were told that memory would be tested for all scenes following the study phase (i.e., intentional
233 encoding). Numeric stimuli were randomly selected from the integers 1-864 and presented in white font
234 for 2 s. Subjects used a button response to indicate if the number was even (right hand button) or odd
235 (left hand button). Visual stimuli were randomly assigned to either a study trial stimulation condition or to
236 serve as a lure during memory testing (see below) for each subject. Stimuli were presented in the center
237 of an MRI-compatible LCD screen (Nordic Neuro Lab, Bergen, Norway) positioned at the subjects' feet,
238 on a gray background, viewed via a mirror attached to the head coil. Responses with hand-held fiber
239 optic button boxes (Current Designs, Inc., Philadelphia, PA, USA). Subjects were told that they could
240 make their responses during the white fixation cross following each stimulus and that response times
241 were not important (i.e., self-paced responses).

242 Stimulation was delivered for ~2 s (see TMS/fMRI acquisition methods for exact timing)
243 immediately preceding stimulus onset for 66% of scene and numeric trials (i.e., stimulation presence on),
244 with no stimulation for the remaining trials (i.e., stimulation presence off). Long inter-trial intervals (11-
245 19.5 s) were used to reduce stimulation carry-over effects (Huang et al., 2005). During one study phase
246 stimulation targeted the hippocampal network via left parietal cortex (HNT), and during the other study
247 phase stimulation targeted the SMA, with a break of ~10 min between study phases for TMS coil
248 repositioning. The order of these conditions was counterbalanced across subjects. Prior to getting in the
249 scanner for the study phases, MRI-navigated TMS software (Localite GmbH, St. Augustin, Germany)
250 was used to physically mark the individualized stimulation locations on the participant's scalp. A
251 conformable MRI-compatible marker was affixed to the scalp at the intended stimulation location (12.7
252 mm x 12.7 mm re-sealable plastic bag filled with yellow-mustard MRI contrast agent; Plochman, Inc.,

253 Manteno, IL, USA). The markers were used to position the TMS coil against the subject's head in the
254 scanner and coil location was recorded via MRI anatomical scans during each study phase (see below).
255 One experimental session used TBS and the other used beta TMS, administered in
256 counterbalanced order across subjects. For both stimulation patterns, 30 TMS pulses were delivered
257 during the 2 s prior to stimulus onset per trial, delivered at the same intensity for each subject (80%
258 RMT). For TBS, pulses were delivered as 50 Hz triplets at 5 Hz. For beta stimulation, pulses were
259 delivered individually at 12.5 Hz. TMS pulses were synchronized with the MRI scan and with visual
260 stimulus onset (see below). To acclimate subjects to the stimulation protocols and to ensure that
261 stimulation did not cause scalp/facial twitches, a train of stimulation was applied once the subject was
262 positioned inside the scanner and the TMS coil was positioned at the targeted location before scanning
263 in each study phase. Stimulation intensity was lowered during one or both sessions due to technical
264 limitations for 5 subjects. On average, TBS was delivered at 78.8% RMT (SD=1.9, range=75.0-80.0) and
265 beta stimulation was delivered at 78.5% RMT (SD=2.2, range=74.1-80.0). The experimental sessions
266 were scheduled at least two days apart, with an average of 27 days between sessions (range=3-84
267 days). For 1 subject, a session was discarded due to technical difficulties and the subject returned for a
268 third "replacement" session. The replacement session was performed with the same location and pattern
269 order as the discarded session, but with different visual stimuli.
270 At the end of each experimental session, memory was tested for the scenes that were presented
271 during both of the study phases for that session (one study phase with HNT stimulation and one with
272 SMA stimulation). After completing both study phases, subjects rested out of the scanner for ~15 min
273 before taking the memory test, which was not scanned. The 144 scenes presented during the study
274 phases were presented one at a time intermixed randomly with 144 novel lures that were not presented
275 during study phases, in randomized order. Subjects responded with (i) "Remember" if they specifically
276 recalled details about seeing the scene, (ii) "Familiar" if they recognized the scene but could not
277 specifically recollect seeing it, and (iii) "New" if the scene was a lure (Yonelinas, 2002; Eichenbaum et al.,
278 2007). Trials were self paced, with the scene remaining on the screen until a response was registered.
279 The duration of the test phases was 20.8 min on average (range=14-29, SD=4.48).
280

Simultaneous TMS/fMRI acquisition

MRI was performed during study phases using a 3T Siemens PRISMA scanner with a single-channel transmitter/receiver head coil. Fast low-angle shot (FLASH) anatomical scans were collected between study phases to localize the actual location of the TMS coil relative to markers placed on the scalp, including a T1 sagittal (50 slices; TE 2.42 ms; TR 311.0 ms; flip angle 80°; 1.0 mm inplane resolution; 4.0 mm thick sagittal slices with 0 mm gap; 50% phase oversampling; 256x256 mm FOV; scan duration 44 sec) and a T1 oblique axial (40 slices; TE 2.42 ms; TR 249.0 ms; flip angle 80°; 1.0 mm inplane resolution; 4.0 mm thick axial slices with 0 mm gap; 60% phase oversampling; 256x256 mm FOV; scan duration 36 sec). These anatomical scans were later used to localize the TMS coil targeting displacement (see below).

We developed two fMRI scan sequences to interface with TMS pulses for the TBS and beta-patterned stimulation conditions. Task-based functional images were acquired using a BOLD contrast sensitive gradient echo EPI pulse sequence that contained custom programmed temporal gaps interleaved between slice acquisitions. Rather than delivering stimulation during slice acquisition, which causes TMS-induced artifact that requires volumes to be discarded (Bestmann et al., 2008; Siebner et al., 2009), TMS was delivered between MRI slice acquisitions during the inserted temporal gaps. This TMS-fMRI method did not cause artifact beyond that associated with the physical presence of the TMS coil, which produces stable artifact near the coil (see Results).

For both stimulation patterns, 30 pulses were delivered during the imaging volume immediately prior to visual stimulus onset for conditions that involved stimulation. Pulses were delivered over a duration of 2000 ms in the TBS condition (Fig. 2A) and 2400 ms in the beta-patterned stimulation condition (Fig. 2B), for a total of 5760 pulses aggregate over the entire experimental session. For TBS, 107-ms temporal gaps were inserted after every two EPI slices (93 ms). During this temporal gap, a 50 Hz triplet burst (pulse every 20 ms) was delivered, with one triplet burst delivered every 200 ms during such temporal gaps (665 frames; TE 20 ms; TR 2230.0 ms; 2442 Hz/pixel bandwidth; flip angle 90°; voxel resolution 3.0 mm isotropic; 22 interleaved 3.0 mm thick axial slices angled to AC-PC alignment and centered on the longitudinal axis of the temporal lobes; 50% phase oversampling in the phase-encoding direction; 192x192 mm FOV; scan duration 24.83 min; 72 trials per scan) (Fig. 2A). For beta-

patterned stimulation, 34-ms temporal gaps were inserted after each slice (46 ms), in which a single TMS pulse could be delivered, such that one pulse was delivered every 80 ms during such temporal gaps (270 frames; TE 20 ms; TR 2440.0 ms; 2442 Hz/pixel bandwidth; flip angle 90°; voxel resolution 3. mm isotropic; 30 interleaved 3.0 mm thick axial slices angled to AC-PC alignment and centered on the longitudinal axis of the temporal lobes; 50% phase oversampling in the phase-encoding direction; 192x192 mm FOV; scan duration 28.38 min; 72 trials per scan) (Fig. 2B). The scans were programmed such that the last TMS pulse would occur at the end of the TR (i.e., all pulses during the final 2000 ms of the 2230 ms TR for the TBS scan and during the last 2400 ms of the 2440 ms TR of the beta-patterned stimulation scan). Phase oversampling in the phase-encoding direction was used in both scans to shift any Nyquist ghosting induced by the presence of the TMS coil outside the brain.

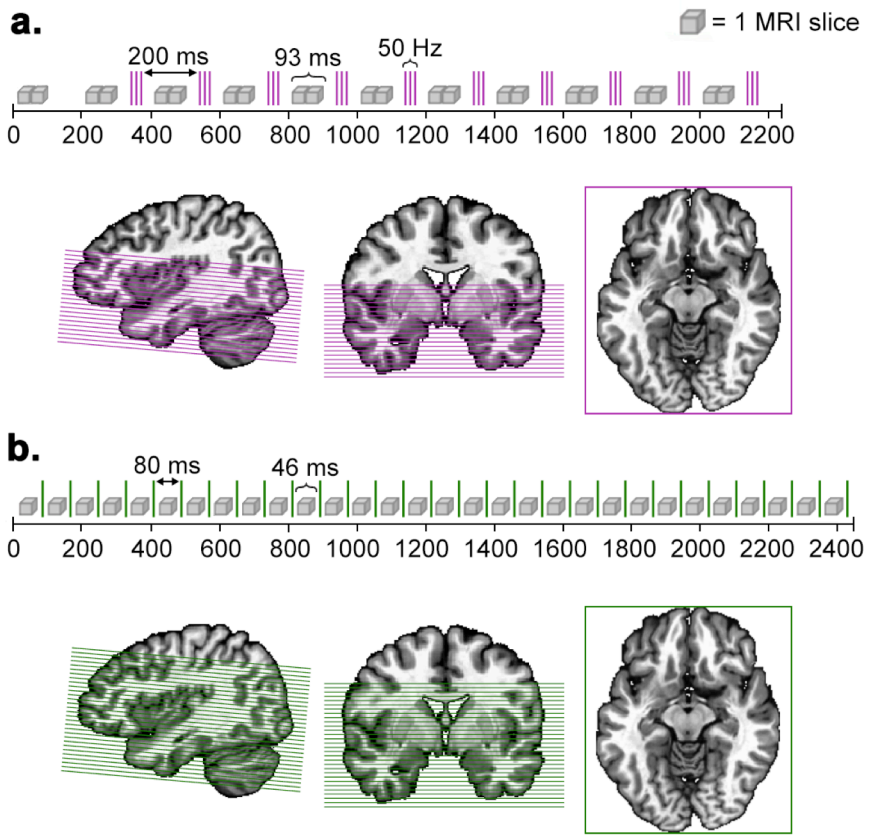

Figure 2. Interleaved TMS/fMRI scan sequences. Depiction of one imaging volume in the (A) TBS and (B) beta scan sequences. Each grey cube represents one MR EPI slice acquisition and each colored line indicates a TMS pulse (purple for TBS; green for beta). The extent of imaging coverage (22 EPI slices for TBS; 30 EPI slices for beta) is shown on a template brain, with EPI slices colorized to match the TMS pulses (purple for the TBS scan; green for the beta scan).

The limited coverage in both the theta- and beta-patterned task-based scans precluded whole-brain imaging but did adequately cover MTL regions of interest when the imaging volume was centered at the MTL (Fig. 2AB). Notably regions imaged directly under/around the TMS coil typically exhibit irreparable TMS-induced artifacts (Bestmann et al., 2008; Siebner et al., 2009), but the parietal cortex and SMA stimulation locations did not fall within our limited coverage. Our hypothesis-driven regions of interest were instead in downstream regions distant from the stimulation location. We confirmed image quality by subject-level visual inspection, as well as validating signal quality at the group-level (see Results). Two task-based scans using the same parameters were acquired per the two study phases during each experimental session (~70 min per phase, 144 trials per phase). Participants wore air-conduction earplugs during the scans to attenuate both scanner and TMS noise.

A PC in the MRI control room received transistor-transistor logic (TTL) pulses from the MR scanner and, based on the experiment code, then sent TTL pulses to the TMS device to trigger stimulation at appropriate times. TTL pulses were sent per EPI slice acquisition to the experiment control PC, which in turn triggered the TMS device to deliver the programmed stimulation sequence. Thus, stimulation delivery was trial-specific and time-locked to the slice-based MR trigger. During the study phases, experiment events (e.g., pulse signals from the MRI and TMS, stimulator settings, participant responses, task stimuli, etc.) were monitored and recorded in output files created by Presentation (Neurobehavioral Systems, Inc. Berkeley, CA, USA), MagVenture (MagVenture A/S, Farum, Denmark), and LabChart (ADInstruments, Inc. Colorado Springs, CO, USA), as well as by the experimenter in the MRI control room. These records were used by the experimenter to update copies of raw output files with trial-specific deviations (i.e., trials were discarded if only part of the stimulation train was delivered due to coil over-heating; records reflected that the trial condition changed from ‘ON’ to ‘OFF’ if stimulation failed entirely during the 2-s pre-stimulus period).

TMS coil displacement during fMRI

We used FLASH anatomical MRI scans (see above) collected before and after the study phase fMRI scans to evaluate the actual location of the TMS coil during the experiment relative to its intended location to account for possible displacement. The scans were uploaded into the MRI-navigated TMS

348 software (Localite GmbH, St. Augustin, Germany) and aligned to the subject's high-resolution anatomical
349 scan collected during the baseline session. We utilized contrast-agent markers on the TMS coil (vitamin
350 E capsules and oil-filled tubing) and on the scalp (mustard packets) to identify the position, orientation,
351 and rotation of the TMS coil inside the scanner (i.e., 4D Matrix of coordinates) relative to the target that
352 was identified based on resting-state fMRI for each subject (see above). The matrices were transformed
353 with a displacement vector to estimate the cortical coordinates directly under the TMS coil. The across-
354 participant mean MNI coordinates of the achieved HNT location was -50, -52, 32 (SD=4.8, 6.7, 6.8) for
355 the TBS session and -49, -51, 33 (SD=4.8, 7.7, 7.3) for the beta stimulation session. The SMA location
356 was -31, -16, 66 (SD=5.4, 9.0, 3.7) for the TBS session and -32, -13, 63 (SD=6.0, 9.3, 5.5) for the beta
357 stimulation session. For each participant and condition, the deviation in achieved versus intended
358 stimulation locations was calculated as the Euclidean distance. For the TBS and beta-patterned
359 sessions, there was an average deviation of 8.47 mm (SD=4.04) for the HNT condition and a deviation of
360 9.02 mm (SD=4.12) for the SMA condition. The amount of deviation did not significantly vary between
361 the two locations (P>0.7).

362 To confirm that the HNT and SMA conditions differentially targeted the hippocampal network as
363 intended despite the in-scanner coil displacement, we analyzed resting-state fMRI connectivity of the
364 achieved stimulation location (considering displacement) with the hippocampal network. Using the high-
365 resolution resting-state fMRI scan collected at baseline, we calculated the hippocampal network as
366 regions with robust connectivity to the left hippocampus (defined as 2-mm spherical segments centered
367 at MNI coordinates: -23, -10, -21; -26, -14, -20; -30, -18, -18; -31 -22 -14; -30, -26, -12; see below for
368 description of these locations in the task-based fMRI analysis). The hippocampal functional connectivity
369 map for each subject was created by correlating (Pearson's *r*) the spatially averaged time series of these
370 hippocampal coordinates with every voxel's time series (*3dTcorr*). A Fisher's *z* transformation was
371 applied to yield a normally distributed correlation map for each subject (*3dcalc*). Group-level voxel-wise
372 analysis of these connectivity maps using one-sample one-tailed *t*-tests (*3dttest++*) identified clusters of
373 contiguous voxels with robust connectivity to the hippocampal seed mask (300+ voxels with *z(r)*
374 significantly greater than 0; t-threshold=5.2; P<0.0001). These clusters were saved as a hippocampal
375 network mask (*3dclust*; 6,695 voxels total). For each subject, we then assessed resting-state connectivity

between the achieved stimulation location to every voxel in the hippocampal network mask (*3dTcorr*) and spatially averaged the correlation value to obtain one overall network connectivity value for each stimulation condition for every subject (*3dmaskave*). A 2x2 repeated measures ANOVA testing the effects of stimulation location and pattern on connectivity to the hippocampal network indicated significant variation by location ($F_{1,12}$=4.83, P=0.04, η^2_p=0.24), such that connectivity was significantly greater for the HNT locations (mean=0.15, SD=0.12) relative to the SMA locations (mean=0.06, SD=0.07) (Fig. 1C). Thus, differential targeting of the hippocampal network by the HNT and SMA locations was successful despite coil displacement during fMRI scanning.

Subject-level task-based fMRI processing

Anatomical scans were skull-stripped (*3dSkullStrip*) and co-registered to the Colin27 template (*auto_tlrc*). Preprocessing of the functional volumes included outlier suppression (*3dDespike*), slice timing and motion correction (*3dvolreg*), and co-registration to the anatomical scan (*align_epi_anat*). The transformations were applied simultaneously in a single resampling step (*3dAllineate*). Motion parameters were calculated for each volume as the Euclidean norm of the first difference of six motion estimates (three translation and three rotation). Volumes with excessive motion (>0.3 mm), as well as the previous volume, were flagged for censoring during the regression analyses, which is a typical threshold for task-based fMRI analysis. On average, 2.8% (SD=5.0) of the TBS HNT condition, 3.6% (SD=6.1) of the TBS SMA condition, 5.0% (SD=8.0) of the beta HNT condition, and 5.9% (SD=10.2) of the beta SMA condition time series were motion censored. There was no significant difference in the amount of censoring across conditions (all pairwise comparison *Ps*>0.10). Data were spatially smoothed using a 6-mm full-width-at-half-maximum (FWHM) isotropic Gaussian kernel (*3dmerge*) and signal intensity was normalized by the mean of each voxel. Task-based masks were created that consisted only of voxels in the brain with stable signal across the scanning sessions (*3dAutomask*).

Two general linear models (GLMs) incorporating hemodynamic response deconvolution were applied to the preprocessed data to estimate voxel-wise event-related activity regression coefficients for each trial type, separately for each stimulation condition (HNT TBS, SMA TBS, HNT beta, and SMA beta) (*3dDeconvolve)*. GLMs were constructed separately per condition because differences in the scan

404 parameters required for TBS versus beta stimulation precluded concatenation of all conditions into one
405 GLM. In each GLM, trials were separated based on experiment condition (scenes with TMS ON, scenes
406 with TMS OFF, numbers with TMS ON, and numbers with TMS OFF). In a second GLM, the scene trials
407 were further sorted by subsequent memory performance (Remember, Familiar, or New responses during
408 the test). Time points with motion spikes and time series outliers were censored. Polynomial trends and
409 motion estimates and their derivatives were included as nuisance regressors of no interest. Condition-
410 specific activity estimates used the duration-modulated gamma function. Each condition of interest (HNT
411 TBS, SMA TBS, HNT beta, and SMA beta) was modeled, with each event beginning at the stimulus
412 (scene or number) onset. Restricted Maximum Likelihood (REML) estimation methods were used to
413 generate voxel-wise parameter estimates and measures of variability for each trial type for each
414 stimulation condition (*3dREMLfit*). Parameter estimates from each subject were later analyzed at the
415 group-level (see below)
416
417 Data analysis
418 *Memory performance*
419 Performance on the scene recognition test was computed as the rate of hits ("Remember" and
420 "Familiar" responses for studied scenes) and correct rejections ("New" response for novel lures) for each
421 subject separately for every stimulation condition. To evaluate stimulation effects on hippocampal-
422 dependent recollection, we calculated the proportion of hits that were recollected ("Remember"
423 responses) for every stimulation condition.
424
425 *Group-level task-based fMRI analyses*
426 Voxel-wise analyses were performed in order to confirm that our scan parameters provided
427 sensitivity to expected fMRI correlates of cognitive processing (i.e., scenes but not numbers should
428 evoke activity in parahippocampal, fusiform, and occipital regions (Stern et al., 1996; Stark and Squire,
429 2001) and stimulation sensations (i.e., sound emitted by stimulation should evoke activity in auditory
430 cortex). The first contrast compared BOLD activity evoked by task stimuli (scenes versus numbers)
431 regardless of stimulation presence, location, or pattern; and the second contrasted activation due to

stimulation presence (on versus off) regardless of stimuli type or stimulation location or pattern. Subject-level GLMs were used to estimate voxel-wise event-related activity regression coefficients for each trial type (i.e., scenes, numbers, TMS ON, and TMS OFF) and REML estimation methods were used to generate voxel-wise parameter estimates and measures of variability for each subject (*3dDeconvolve, 3dREMLfit; see above*). GLM maps were analyzed at the group-level using generalized least squares with a local estimate of random effects variance (*3dMEMA*) to identify regions of significant difference ($P<0.001$, t-threshold=4.07) for scenes versus numbers and for stimulation on versus off. Data from theta-patterned and beta sessions were analyzed separately due to the differences in scan parameters.

To test whether differences in parameters between the TBS and beta stimulation scans did not significantly affect the signal quality, the Signal-to-Fluctuation-Noise Ratio (SFNR) summary value (Friedman and Glover, 2006) was assessed and compared between the two fMRI sequences. The mean signal was divided by the standard deviation of the residuals (*3dTstat, 3dcalc)* and then averaged within the limited task coverage mask over the whole session (*3dmaskave*) to yield one TSNR value per stimulation condition per subject.

To measure the effect of stimulation on activity during the memory task, performance on the retrieval task was used to back-sort fMRI data to analyze the effects of stimulation on encoding-related activity that predicted subsequent recollection (trials that were later endorsed with “Remember” responses). Subject-level GLMs estimated voxel-wise event-related activity regression coefficients for each trial type (i.e., remembered scenes with TMS ON, remembered scenes with TMS OFF, scenes not-recollected with TMS ON, scenes not-recollected with TMS OFF, numbers with TMS ON, and numbers with TMS OFF) for each stimulation condition (*3dDeconvolve, 3dREMLfit*; see above*)*. For stimulation conditions with “Remember” responses, there were 16 trials on average (range=6-33) per condition (trial counts did not vary by condition $P>0.2$). Trials with remembered scenes with TMS OFF were collapsed across all study sessions to create the “combined off” condition (average number of trials=27, range=15-46). Similarly, activity for numeric judgment trials was estimated, but without respect to test performance (i.e., all trials), separately for each stimulation condition, and collapsed across all study sessions for the “combined off” condition.

The influence of stimulation conditions on fMRI activity estimates for remembered scenes and numeric judgment trials were tested at the group level using 6-mm radius spherical regions of interest (ROIs) along the hippocampal longitudinal axis in each hemisphere. The goal was to identify locations within the MTL that responded to stimulation conditions, taking into account potential functional distinctions along the anterior-posterior MTL axis (Aggleton and Brown, 1999; Ranganath and Ritchey, 2012; Poppenk et al., 2013) as in our previous experiments investigating the effects of TMS on MTL function (Wang et al., 2014; Nilakantan et al., 2019). The middle ROI in the left hemisphere was placed in the body of the hippocampus, centered at the coordinate that was targeted via its connectivity with parietal cortex as measured during the baseline session resting-state fMRI scan (centroid MNI coordinate: -30 -18 -18). Two spheres were placed anterior to this location (centroid MNI coordinates: -23 -10 -21; -26 -14 -20), and two posterior (centroid MNI coordinates: -31 -22 -14; -30, -26, -12), in 4mm increments along the longitudinal axis. These coordinates were mirrored into the right hemisphere (centroid MNI coordinates: 23 -10 -21; 26 -24 -20; 30 -18 -18; 31 -22 -14; 30 -26 -12. The two most anterior spheres encompassed the head of the hippocampus and the middle and two posterior spheres fell in the body of the hippocampus. These spherical ROIs encompassed hippocampal as well as surrounding medial temporal lobe tissue. Spherical ROIs were used in lieu of more anatomically precise methods (e.g., hippocampal subfield identification) due to the limited spatial resolution imposed by the scanning parameters that are possible with the single-channel MRI head coil, which was necessary to accommodate the TMS coil.

Exploratory voxel-wise analysis was used to evaluate whether there were significant effects of stimulation other than in the MTL ROIs. This analysis compared activity estimates for scenes with stimulation that were later recollected between stimulation conditions. Each subject's voxel-wise regression coefficients for remembered scenes with TMS ON for every stimulation condition (HNT TBS, SMA TBS, HNT beta, SMA beta) was entered into repeated measures ANOVA (*3dANOVA3*) to assess voxels for a significant interaction between stimulation location and pattern. Clusters of significant interaction were identified using a liberal threshold (two-tailed $P<0.05$ voxel-wise threshold, t-stat=1.96, >40 contiguous supra-threshold voxels) (*3dClust*). Follow-up pairwise comparisons were made of the main condition of interest (HNT TBS) versus the stimulation location control (SMA TBS) and versus the

487 stimulation pattern control (HNT beta) (*3dttest++*). For each contrast, clusters of voxels were identified
488 using a liberal threshold (two-tailed P<0.05 voxel-wise threshold, t-stat=1.96, >40 contiguous supra-
489 threshold voxels) (*3dClust*) and saved as a mask to visualize the intersection of the thresholded
490 statistical maps.
491
492 Statistics
493 Statistical analysis was performed using AFNI and Matlab. Group-level analysis of multiple
494 conditions was performed using repeated-measures factorial analysis of variance (rmANOVA), with
495 partial eta squared (η^2_p) reported as the effect size. Greenhouse-Geisser correction was applied if the
496 assumption of sphericity was not met (significant Mauchly's test at P<0.05), with the corrected p-values
497 and degrees of freedom reported ($F_{(GG)}$). Pairwise comparisons were made using Students t-tests (t) or
498 Wilcoxon signed rank tests (z) if the assumption of normality was violated (significant Shapiro-Wilk test at
499 P<0.05). Effect size measures were calculated as Cohen's *d* (*d*) for the t-tests and as rank-biserial
500 correlation (*r*) for the Wilcoxon tests. All statistical tests were paired/within-subjects and were two-
501 sided/tailed. Results are indicated as significant at *P < 0.05, **P < 0.01, ***P < 0.001.
502
503 Data and materials availability
504 Raw data are freely available on the Northwestern University Neuroimaging Data Archive
505 (https://nunda.northwestern.edu/). Dataset identifiers will be provided with publication to permit
506 unrestricted access to raw data. Custom code and scripts to replicate analyses will also be available via
507 this archive.
508
509 **Results**
510 Validation of concurrent TMS-fMRI
511 The fMRI scanning methods used for TBS and beta stimulation differed in a number of critical
512 parameters, including parameters of the scan sequence as well as the timing of scan acquisition relative
513 to interleaved TMS pulses (Fig. 2AB). To test whether these differences affected signal quality, the
514 Signal-to-Fluctuation-Noise Ratio (SFNR) summary value (Friedman and Glover, 2006) was calculated

515 for each subject for the TBS and beta stimulation sessions. We expected SFNR values to be ~120, as
516 this was the approximate SFNR value obtained when we performed the same scans on an additional
517 subject who had the TMS coil at the same approximate locations but without any pulses delivered
518 (average SNFR across both scans = 120.3). Furthermore, another group using the same scanner and
519 head coil models as in this experiment reported similar SFNR values for their interleaved TMS/fMRI
520 scans (Moisa et al., 2009). The average SFNR value for the TBS sessions was 122.5 (SD=18.3,
521 range=94.8-160.2) and 123.4 for the beta sessions (SD=14.2, range=92.2-144.8), with no significant
522 difference between sessions (P=0.75). Therefore, scan stability and thus, sensitivity, did not vary by scan
523 sequence or stimulation pattern.

524 We performed two voxel-wise fMRI analyses to confirm expected neural activity correlates of
525 cognitive processing within the task. That is, scenes but not numbers should evoke activity in
526 parahippocampal, fusiform, and occipital regions (Stern et al., 1996; Stark and Squire, 2001) and
527 stimulation sensations such as TMS sounds should evoke activity in auditory cortex. The contrast of fMRI
528 activity evoked by scenes versus numbers, calculated across stimulation presence (on and off), and
529 location (HNT and SMA) identified significantly greater activity (P<0.001, t-threshold=4.07) of bilateral
530 occipital, fusiform, and posterior parahippocampal cortex as well as hippocampus for both stimulation
531 patterns (Fig. 3A). Contrasts between TBS and beta stimulation identified no voxels with significant
532 differences even at a liberal threshold (P<0.01 uncorrected). The contrast of stimulation “on” versus “off”,
533 calculated across stimulation location (HNT and SMA), identified significantly greater activity for “on”
534 (P<0.001, t-threshold=4.07) in bilateral auditory cortex for both TBS and beta stimulation (Fig. 3B).
535 Again, the direct contrast identified no voxels with significantly different activity for TBS versus beta
536 stimulation at a liberal threshold (P<0.01 uncorrected). Notably, although auditory-related activity due to
537 stimulation was identified robustly, the limited imaging volume did not permit identification of likely
538 somatosensory activation. Collectively, these analyses indicate that fMRI sensitivity was sufficient for
539 identifying typical neural signals of scene viewing and auditory stimulation despite concurrent TMS and
540 that there was no obvious variation in sensitivity for TBS versus beta scan parameters.

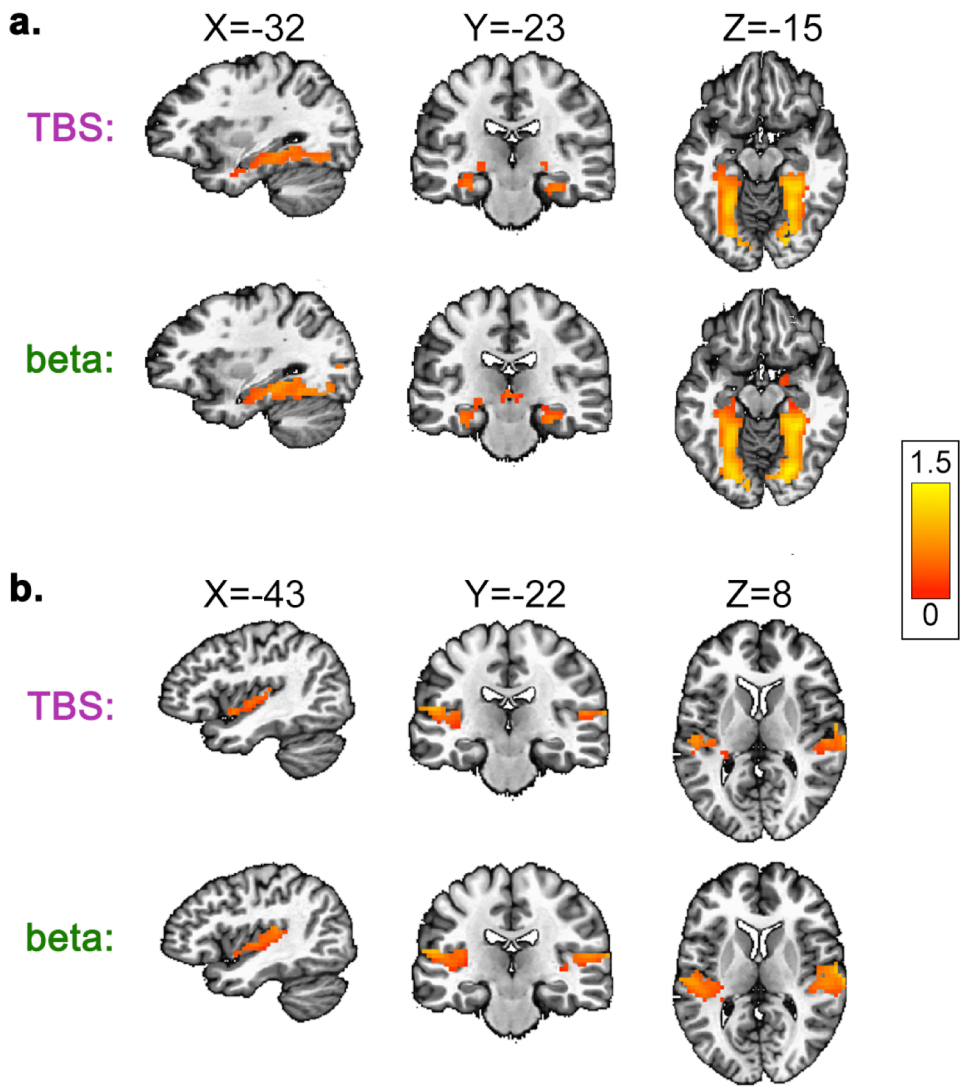

Figure 3. Expected fMRI signals of scene processing and stimulation sensations confirm fMRI data quality during concurrent TMS. Voxel-wise contrasts confirm that the fMRI signal could distinguish the task stimuli (scenes vs. numbers) and the presence of stimulation (ON vs. OFF). (A) Group-level contrast of scenes versus numbers, regardless of stimulation location or presence, identified significantly greater activation by scenes in the bilateral occipital, fusiform and posterior parahippocampal gyri for both TBS and beta stimulation. (B) Group-level contrast of TMS ON versus OFF, regardless of stimulation location or the stimuli type (scenes and numbers) identified significantly greater activation for TMS ON in the bilateral auditory cortex for both TBS and beta stimulation. Direct contrasts of TBS versus beta did not identify significant differences for either comparison (see main text). Plots show supra-threshold voxels on a template brain. Color bar indicates group mean percent signal change estimated by *3dMEMA*.

541

542 Effects of stimulation on memory encoding

543 We hypothesized that subsequent recollection of scenes that were stimulated during encoding
544 would increase due to HNT TBS relative to all control stimulation conditions. Consistent with this
545 prediction, the proportion of retrieval hits endorsed with recollection responses during the memory test
546 that followed scanning (Fig. 4A) varied significantly by stimulation presence (on versus off), pattern (TBS
547 versus beta), and location (HNT versus SMA) (3-way interaction $F_{1,11}$=6.63, P=0.02, η^2_p=0.44) during
548 encoding. This reflected more recollected hits for scenes preceded by HNT TBS relative to other
549 conditions (Table 1; Fig. 4B). Post-hoc pairwise comparisons (Fig. 4B) indicated that the proportion of
550 recollected hits was greater for HNT TBS versus the corresponding "off" condition (t_{15}=2.78, P=0.01,
551 d=0.74), versus SMA TBS (matched-frequency location control: t_{15}=4.11, P=0.0009, d=1.13), and
552 marginally greater versus HNT beta (matched-location frequency control: t_{15}=1.97, P=0.07, d=0.50). In
553 contrast, none of the other stimulation conditions increased recollection relative to the "off" condition (all
554 Ps>0.1; Fig. 4B).

555 Although it might be reasoned that evidence for effects of stimulation on memory should be
556 obtained by comparing a particular stimulation condition versus a corresponding stimulation "off"
557 condition, this comparison is problematic because stimulation can have a variety of nonspecific disruptive
558 or enhancing effects on cognition (i.e., distraction, arousal, etc.). Likewise, TBS and beta stimulation vary
559 in somatosensory and auditory qualities, which could produce distinct effects on memory for nonspecific
560 reasons. Therefore, a rigorous way to test for differential effects of stimulation patterns on recollection is
561 to contrast the effects of TBS versus beta stimulation when each type of stimulation targeted the
562 hippocampal network (HNT) versus the SMA. This is because TBS is subjectively similar for HNT versus
563 SMA, as is beta stimulation, yet these locations vary in their expected effect on memory processing. The
564 relative recollection advantage for HNT versus SMA stimulation was greater for scenes in the TBS
565 condition relative to scenes without stimulation ("off") in the TBS session (t_{15}=3.48, P=0.003, d=0.87),
566 relative to scenes in the beta stimulation condition (t_{15}=2.26, P=0.04, d=0.57), and relative to scenes
567 without stimulation in the beta session (t_{15}=2.75, P=0.01, d=0.69) (Fig. 4C; subject-level differences for
568 each comparison is provided in Fig. 4D). Thus, recollection was enhanced only by HNT TBS, and this
569 enhancement likely was not due to nonspecific sensory qualities of stimulation pattern.

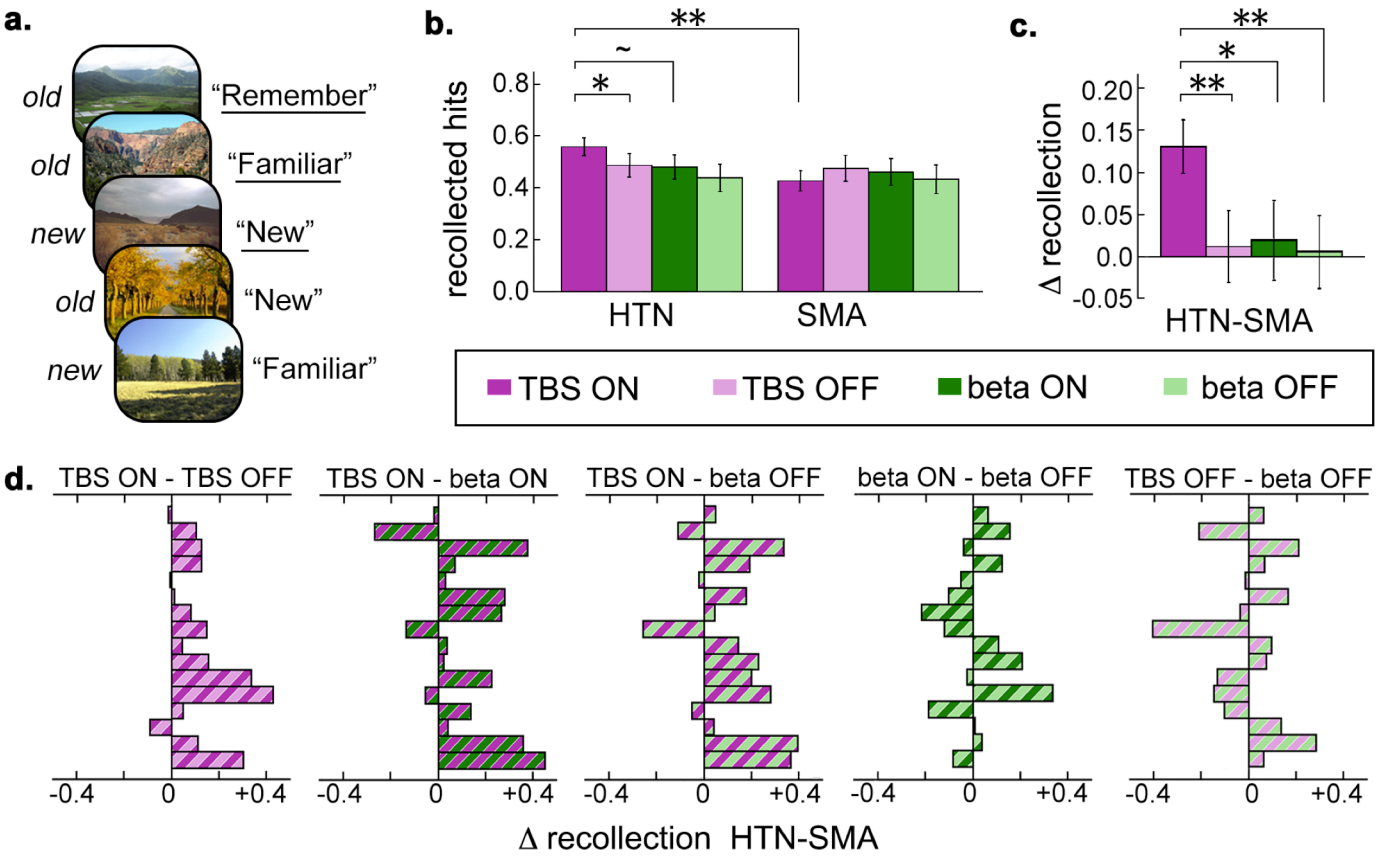

Figure 4. Theta-patterned stimulation of the hippocampal network selectively increased recollection memory. (A) Subjects discriminated studied scenes (old) from randomly intermixed novel lures (new) using "Remember" responses to indicate the experience of hippocampal-dependent recollection, "Familiar" responses to indicate the experience of familiarity, and "New" responses to indicate lures. Example correct responses are underlined. (B) Mean + s.e.m. proportion of recollected hits for each stimulation condition. (C) To identify stimulation effects on memory while holding subjective qualities relatively constant, we compared the difference in the proportion of recollected hits for stimulation targeting HIP versus SMA for each of the stimulation patterns (theta, beta, and off). Mean HTN – SMA differences ± s.e.m. for each condition are in black. (D) Subject-level differences for each comparison of HTN-SM, as shown at the group level in Fig. 4C. * P<0.05, ** P<0.01 by two-tailed t-test.

570

571 The effects of stimulation on memory were specific to hippocampal-dependent recollection, as
572 stimulation did not influence overall hit rates. Overall hit rate (old items endorsed with “Remember” and
573 “Familiar” responses) did not vary by stimulation pattern, location, or presence (all 3-way rmANOVA main
574 effects and interactions P values>0.1) (Table 1). Notably however, although effects of stimulation on hit
575 rates were not identified, overall memory strength could have been affected by stimulation, which could
576 influence both the hit rate and the false alarm rate. The format of the experiment precluded calculation of
577 false alarm rates separately for each stimulation condition because study phases for both stimulation
578 locations (HNT and SMA) were tested at the end of each experimental session using the same set of
579 novel lures (see Fig. 1D). Therefore, lures could be segregated based on stimulation pattern (TBS versus
580 beta) but not based on stimulation location. The false alarm rate was significantly lower (t_{15}=2.54,
581 P=0.02, d=0.64) for TBS (mean=0.31, SD=0.17) than beta stimulation (mean=0.38, SD=0.12),
582 suggesting that TBS increased overall memory strength to a greater extent than beta stimulation.
583
584 <u>Effects of stimulation on medial temporal lobe activity</u>
585 Successful memory formation is associated with relatively increased fMRI activity in the MTL
586 (Paller and Wagner, 2002; Kim, 2011). We therefore hypothesized that HNT TBS would increase MTL
587 fMRI activity evoked by scenes that were later recollected relative to control conditions. Stimulation
588 effects on activity were assessed in spherical segments extending along the hippocampal longitudinal
589 axis and including adjacent rhinal/parahippocampal cortex (Fig. 5A), as relatively large imaging voxels
590 were required given constraints on scan parameters (see Materials and Methods). Stimulation targeted
591 the left hippocampus/MTL via resting-state functional connectivity (Materials and Methods) and based on
592 the relatively lateralized projections from lateral temporal cortex to ipsilateral medial temporal lobe
593 (Mesulam et al., 1977; Mufson and Pandya, 1984). Thus, segments of the right hippocampus/MTL
594 served as non-targeted controls.
595 For left MTL segments, activity varied significantly by the five stimulation conditions (HNT TBS,
596 SMA TBS, HNT beta, SMA beta, and “off”) (main effect $F_{4,375}$=3.29, P=0.02, η^2_p=0.22). Follow-up tests
597 among stimulation conditions made for each MTL segment indicated that activity varied significantly by
598 stimulation condition for the two most anterior left segments ($F_{(GG)1.92,35.97}$=4.14, P=0.03, η^2_p=0.28;

599 $F_{(GG)1.73,32.37}$=3.80, P=0.04, η^2_p=0.25; all other Ps>0.1) (Fig. 5A). Activity of these two anterior segments
600 was significantly greater for HNT TBS relative to HNT beta (Wilcoxon z=3.15, P=0.002, r=0.51), SMA
601 TBS (Wilcoxon z=2.95, P=0.003, r=0.54), SMA beta (Wilcoxon z=2.48, P=0.01, r=0.62), and the "off"
602 condition (Wilcoxon z=1.96, P=0.04, r=0.49) (Fig. 5B). Activity was significantly lower for SMA TBS
603 relative to the "off" condition (Wilcoxon z=2.33, P=0.02, r=0.58) (Fig. 5B), suggesting that TBS out of the
604 hippocampal network may have disrupted hippocampal/MTL activity (but see above for an explanation
605 for why comparison to stimulation "off" conditions can be ambiguous). The same analysis performed for
606 right (non-targeted) MTL segments yielded a numerically similar but non-significant pattern of greater
607 activity following HNT TBS relative to other conditions (Ps>0.1) (Fig. 5).

608 As hypothesized, MTL activity evoked by numeric judgments did not vary significantly by
609 stimulation condition in either the left or right hemisphere (Fig. 5; main effect of condition and interaction
610 of condition by longitudinal segment in the left and right hemispheres Ps>0.3). Further, HNT TBS had
611 significantly greater impact on fMRI activity during memory formation than during numeric judgments. For
612 the two anterior left MTL segments with activity that varied by stimulation condition (Fig. 5), the difference
613 in activity evoked by later-recollected scenes minus numeric judgments was significantly greater for HNT
614 TBS relative to HNT beta (Wilcoxon z=2.17, P=0.03, r=0.54) and relative to SMA TBS (Wilcoxon z=2.07,
615 P=0.04, r=0.52). Thus, TBS targeting the hippocampal network was selective in its influence on memory
616 processing relative to numeric processing.

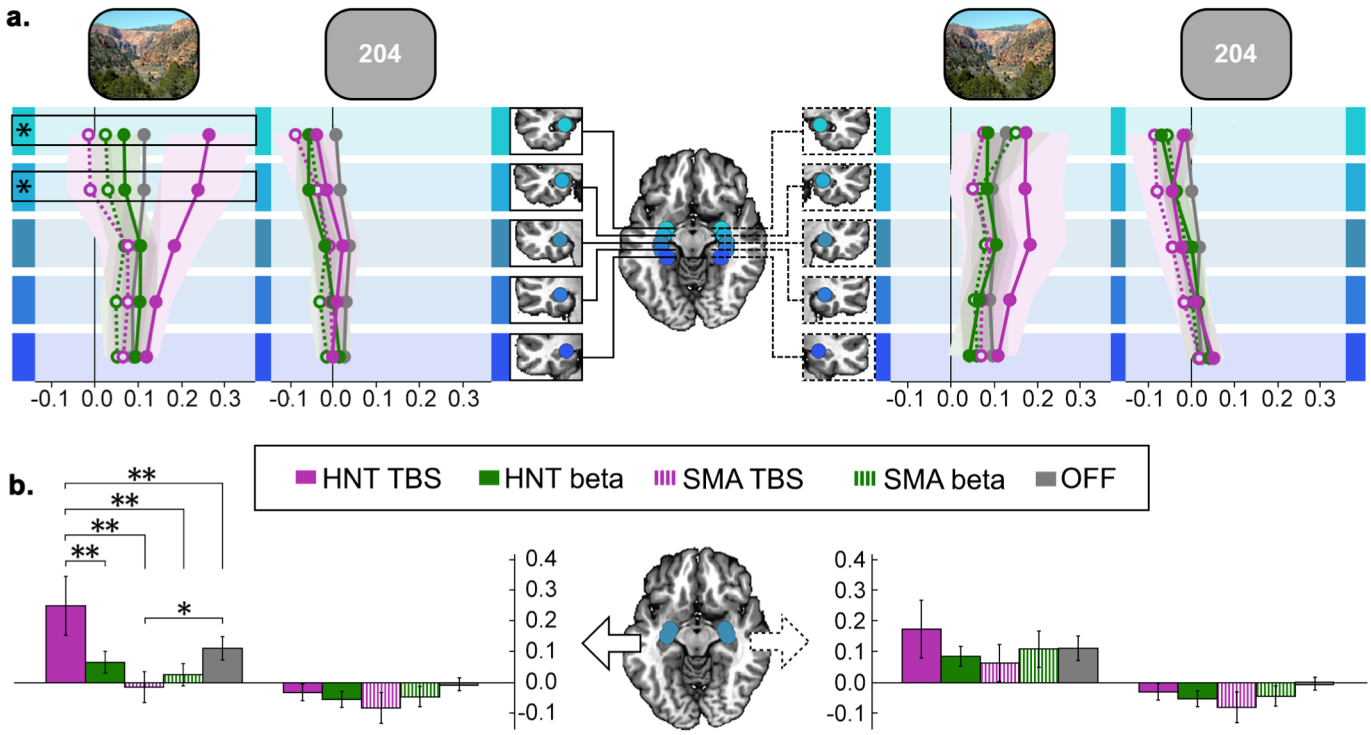

Figure 5. Stimulation targeting hippocampal theta selectively increased hippocampal activity during recollection memory formation. (A) Stimulus-evoked fMRI activity was measured within MTL segments centered along the hippocampal longitudinal axis in each hemisphere, shown as colorized spheres on a template brain. The left hippocampus/MTL was targeted indirectly via its network functional connectivity (Materials and Methods) and the right hippocampus/MTL served as a non-targeted control. Line plots indicate mean estimated fMRI activity (percent signal change) ±s.e.m. (shaded area) during the study phases for each of the five stimulation conditions for trials with scenes that were later recollected and for trials with numeric judgments. *Segments with P<0.05 effects of stimulation condition by five-way rmANOVA are outlined (see text). (B) Mean fMRI activity ±s.e.m. for the same stimulation conditions averaged for the two anterior spherical segments for the left and right MTL for trials with scenes that were later recollected and for trials with numeric judgments. * P<0.05, ** P<0.01 by two-sided paired Wilcoxon signed rank tests.

617

618 Exploratory voxel-wise analysis of stimulation effects on recollection-related fMRI activity

619 To further evaluate whether recollection-related activity during scene encoding for regions outside
620 the MTL was sensitive to HNT TBS versus all control conditions, we conducted a voxel-wise exploratory
621 analysis. A repeated measures ANOVA with a liberal statistical threshold (Methods) identified a cluster of
622 82 voxels in the left anterior MTL (center of mass MNI = -34 -2 -20) with significant interaction between
623 stimulation location and pattern (Fig. 6A). Follow-up pairwise comparisons were made of the main
624 condition of interest (HNT TBS) versus the stimulation-location control (TBS of the SMA) and versus the
625 stimulation-pattern control (HNT beta stimulation). The only region for which these two contrasts
626 intersected (i.e., demonstrated supra-threshold voxels specific to TBS versus beta stimulation and to
627 HNT versus SMA stimulation) was left anterior MTL (19 voxels, center of mass MNI = -30 -3 -21). For
628 both the ANOVA and the overlap of pairwise comparisons, the location identified via this voxel-wise
629 analysis overlapped considerably with the anterior-left hippocampal/MTL regions of interest that showed
630 the same selective response to HNT TBS in the main analysis using ROIs (Figs. 5A, 6B). Thus, the left
631 anterior hippocampus (head) and immediately surrounding medial temporal cortex (entrorhinal/perirhinal)
632 were the only regions identified with recollection-related activity that preferentially responded to HNT
633 TBS.

634

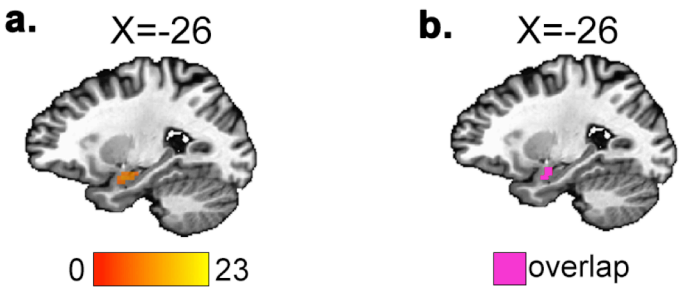

Figure 6. Voxel-wise exploratory analysis of HNT TBS effects on recollection-related activity. Visualization of supra-threshold voxels from the exploratory analyses (see main text). (A) Results from the voxel-wise RM-ANOVA. Color bar indicates F values. (B) Magenta indicates the location of overlap of pairwise tests intended to contrast HNT TBS to control conditions. No other regions besides this left anterior MTL area were identified by either exploratory analysis.

635

636 **Discussion**

637 The key findings of this experiment were that TBS targeting the hippocampal network (HNT)
638 selectively improved memory for stimulated scenes and increased corresponding MTL fMRI activity. A
639 number of aspects of the experiment design and the pattern of results support these key findings. The
640 effects of stimulation on memory and MTL fMRI activity were frequency specific and location specific, in
641 that they were not observed for beta stimulation targeting the hippocampal network nor for either
642 stimulation condition (TBS or beta) targeting an out-of-network control location (SMA). Further, the
643 effects were cognitively specific, in that no stimulation condition (including HNT TBS) influenced MTL
644 fMRI activity during numeric judgments, which do not typically evoke MTL activity (Stark and Squire,
645 2001). This indicates that TBS targeting the hippocampal network only influenced neural correlates of
646 memory processing and provides the strongest evidence that the main findings of HNT TBS on fMRI
647 activity were not due to TMS-related fMRI artefact, as numeric-judgment trials were intermixed with
648 scene-encoding trials and involved the same stimulation parameters and locations. Further, the effects
649 were specific to the left MTL, the hemisphere that was targeted via its connectivity to the left parietal area
650 that was stimulated. A numerically similar but non-significant pattern was observed for right MTL, which
651 could be due to commissural connectivity and is consistent with our previous findings of relatively (but
652 not completely) lateralized effects of network-targeted TMS on the MTL (Wang et al., 2014; Nilakantan et
653 al., 2019). Finally, TBS only influenced the recollective aspect of scene memory, which supports the
654 conclusion that hippocampal function was affected, as recollection is particularly dependent on
655 hippocampus (Eichenbaum et al., 2007; Ranganath and Ritchey, 2012).

656 The immediate effects of TBS targeting the hippocampal network on MTL fMRI activity and scene
657 memory formation suggest that this type of stimulation influenced hippocampal neural activity, as
658 opposed to neuroplasticity and/or neuromodulatory mechanisms that can support persistent/long-lasting
659 effects of stimulation on network function (Cirillo et al., 2017). The premise of the experiment was that
660 TBS mimics the endogenous theta-band neural activity pattern characteristic of the hippocampus and of
661 hippocampal network synchrony (Buzsaki, 2002; Buzsaki and Draguhn, 2004; Lisman and Jensen, 2013)
662 and therefore might optimally influence memory processing via entrainment of neural activity (Thut et al.,
663 2011a; Hanslmayr et al., 2019). Thus, if targeting of hippocampal network theta activity via noninvasive

664 TBS were successful, we expected that it would cause population synchrony of theta and therefore
665 increase the evoked fMRI BOLD response when presented with a visual stimulus that evokes processing
666 by the affected region(s). Although our findings are highly consistent with this prediction, a weakness is
667 that such theta rhythms cannot be measured with fMRI and we can only infer an impact based on the
668 observed pattern of fMRI activity. Confirmation of this interpretation would require direct measurement of
669 stimulation effects on hippocampal theta.

670 Nonetheless, the findings are notable in that they inform understanding of the mechanisms by
671 which noninvasive stimulation influences activity in areas such as the MTL. Noninvasive stimulation
672 targeting the hippocampal network can generate relatively long-lasting aftereffects within the
673 hippocampus and broader hippocampal network (Wang et al., 2014; Kim et al., 2018; Tambini et al.,
674 2018; Freedberg et al., 2019; Hermiller et al., 2019), with greater aftereffects when using theta-burst
675 stimulation (Hermiller et al., 2018). The current findings provide novel mechanistic insights to these
676 previous findings by showing that MTL activity is immediately sensitive to stimulation applied to its
677 network and matching its endogenous theta activity pattern. This suggests an impact of hippocampal
678 network-targeted stimulation on MTL neural activity and supports the interpretation that the effects of
679 noninvasive stimulation targeting this network are due to the impact of stimulation on the MTL (Hebscher
680 and Voss, in press).

681 Although the effects of HNT TBS that we observed were specific to MTL activity, it is noteworthy
682 that sampling of activity elsewhere in the brain was limited by the fMRI methods (Materials and
683 Methods). Nonetheless, we found no evidence for similar effects in regions other than the left medial
684 temporal lobe in an exploratory voxel-wise analysis, and other areas of the hippocampal network were
685 within the volume that was sampled with fMRI (particularly lateral-temporal and medial parietal-occipital
686 cortex) (Fig. 2). This suggests that the MTL may be unique in its ability to be immediately impacted by
687 stimulation. This is consistent with previous evidence that although hippocampal network-targeted
688 stimulation is typically delivered at parietal cortex, the most robust effects of stimulation are on fMRI
689 activity of the hippocampus/MTL and nearby areas of parahippocampal and retrosplenial/medial-parietal
690 cortex (Wang et al., 2014; Kim et al., 2018; Warren et al., 2018; Freedberg et al., 2019). Although the
691 immediate effects of stimulation were limited to the MTL, previous experiments using longer stimulation

692 trains and/or multiple days of stimulation found effects distributed throughout a greater portion of the
693 hippocampal network (Hebscher and Voss, in press). It is possible that brief trains of TBS affect activity
694 in only those areas most sensitive to this stimulation pattern (MTL) whereas more extensive stimulation
695 regimens produce expanded recruitment. This is a direction for future experiments.

696 A limitation of the current experiment is that the memory test was given after both study phases
697 on a given experiment session, and those study phases differed in the location of stimulation (HNT
698 versus SMA), keeping stimulation rhythm constant (TBS or beta). Thus, we could not compare the
699 effects of stimulation location on memory accuracy, as novel foils were not segregated by stimulation
700 location. Nonetheless, we did find reduced false alarms to novel foils for TBS versus beta stimulation as
701 well as an increase in hit rates for TBS delivered to the hippocampal network (HNT) versus to the SMA
702 control location (Table 1). This pattern of findings suggests that HNT TBS potentially increased memory
703 accuracy relative to HNT SMA and to the beta stimulation conditions, but this cannot be confirmed given
704 the limitation of the design. Furthermore, the main analysis strategy (Fig. 4) found that HNT TBS
705 increased the proportion of hits endorsed with recollection responses. Recollection responses typically
706 correlate very highly with memory accuracy (Yonelinas, 2001) and are associated with hippocampal
707 contributions to memory (Eichenbaum et al., 2007; Ranganath and Ritchey, 2012). Thus, TBS targeting
708 the hippocampal network improved recollection, but future experiment will be needed to fully confirm
709 whether memory accuracy can be similarly improved.

710 Although TBS targeting the hippocampal network (HNT) was the only condition that significantly
711 improved memory encoding and increased MTL fMRI activity, the overall pattern of results suggest that
712 other stimulation conditions may have had a negative impact on encoding and MTL fMRI activity. There
713 was numeric but non-significant reduction in the proportion of recollected hits for TBS targeting SMA
714 relative to the corresponding “off” condition (Table 1; Fig. 4B). Furthermore, there was numeric reduction
715 in left MTL activity relative to the “off” condition in all stimulation conditions other than HNT TBS (Fig. 5),
716 and this reduction was significant for TBS targeting SMA. This suggests that stimulation frequencies not
717 well aligned with hippocampal theta could have disruptive immediate effects on MTL memory processing.
718 It is also possible that TMS is simply distracting relative to “off”, particularly for the TBS pattern, and that
719 the beneficial effects of TBS targeting the hippocampal network are sufficient to counteract this negative

720 impact and produce improvement. However, the relative reductions in activity for stimulation conditions
721 other than HNT TBS seemed to be more pronounced for the left (targeted) rather than right (non-
722 targeted) hemisphere, which is inconsistent with explanations involving general factors such as
723 distraction. In either case, the weak reductions in memory and MTL activity for most stimulation
724 conditions stand in contrast to the significant enhancement seen for HNT TBS, suggesting that only this
725 type of stimulation can produce an immediate enhancement of MTL memory processing.

726 Theta oscillations in the hippocampus and surrounding medial temporal lobe could provide a
727 temporal framework for information coding and memory (Buzsaki, 2002) and could support memory-
728 related synchrony among distributed locations of the hippocampal network. Hippocampal network
729 dysfunction is related to memory impairments in a variety of psychiatric, neurological, and
730 neurodegenerative disorders (Andrews-Hanna et al., 2007; Buckner et al., 2008; Dickerson and
731 Eichenbaum, 2010; Small et al., 2011). The current findings suggest that memory processing by the core
732 MTL area of this network can be immediately and beneficially influenced via noninvasive stimulation
733 when stimulation targets the network and is matched to its endogenous activity rhythm. This provides
734 mechanistic insights relevant to the many previous findings of lasting improvements in memory due to
735 noninvasive stimulation targeting the hippocampal network (Hebscher and Voss, in press). Given the
736 immediate impact and relatively precise locus of stimulation-related activity changes, concurrent TBS
737 with fMRI could be a powerful tool for testing a variety of hypothesized MTL contributions to memory and
738 cognition.

References:

Aggleton JP, Brown MW (1999) Episodic memory, amnesia, and the hippocampal-anterior thalamic axis. Behav Brain Sci 22:425-444; discussion 444-489.

Andrews-Hanna JR, Snyder AZ, Vincent JL, Lustig C, Head D, Raichle ME, Buckner RL (2007) Disruption of large-scale brain systems in advanced aging. Neuron 56:924-935.

Battaglia FP, Benchenane K, Sirota A, Pennartz CM, Wiener SI (2011) The hippocampus: hub of brain network communication for memory. Trends Cogn Sci 15:310-318.

Bestmann S, Ruff CC, Blankenburg F, Weiskopf N, Driver J, Rothwell JC (2008) Mapping causal interregional influences with concurrent TMS-fMRI. Exp Brain Res 191:383-402.

Buckner RL, Andrews-Hanna JR, Schacter DL (2008) The brain's default network: anatomy, function, and relevance to disease. Ann N Y Acad Sci 1124:1-38.

Buzsaki G (2002) Theta oscillations in the hippocampus. Neuron 33:325-340.

Buzsaki G, Draguhn A (2004) Neuronal oscillations in cortical networks. Science 304:1926-1929.

Chanes L, Quentin R, Tallon-Baudry C, Valero-Cabre A (2013) Causal frequency-specific contributions of frontal spatiotemporal patterns induced by non-invasive neurostimulation to human visual performance. J Neurosci 33:5000-5005.

Cirillo G, Di Pino G, Capone F, Ranieri F, Florio L, Todisco V, Tedeschi G, Funke K, Di Lazzaro V (2017) Neurobiological after-effects of non-invasive brain stimulation. Brain Stimul 10:1-18.

Coleshill SG, Binnie CD, Morris RG, Alarcon G, van Emde Boas W, Velis DN, Simmons A, Polkey CE, van Veelen CW, van Rijen PC (2004) Material-specific recognition memory deficits elicited by unilateral hippocampal electrical stimulation. J Neurosci 24:1612-1616.

Cox RW (1996) AFNI: software for analysis and visualization of functional magnetic resonance neuroimages. Comput Biomed Res 29:162-173.

Demeter E, Mirdamadi JL, Meehan SK, Taylor SF (2016) Short theta burst stimulation to left frontal cortex prior to encoding enhances subsequent recognition memory. Cogn Affect Behav Neurosci 16:724-735.

Dickerson BC, Eichenbaum H (2010) The episodic memory system: neurocircuitry and disorders. Neuropsychopharmacology 35:86-104.

Eichenbaum H, Yonelinas AP, Ranganath C (2007) The medial temporal lobe and recognition memory. Annu Rev Neurosci 30:123-152.

Ezzyat Y et al. (2018) Closed-loop stimulation of temporal cortex rescues functional networks and improves memory. Nat Commun 9:365.

Fell J, Klaver P, Lehnertz K, Grunwald T, Schaller C, Elger CE, Fernandez G (2001) Human memory formation is accompanied by rhinal-hippocampal coupling and decoupling. Nat Neurosci 4:1259-1264.

Fell J, Ludowig E, Staresina BP, Wagner T, Kranz T, Elger CE, Axmacher N (2011) Medial temporal theta/alpha power enhancement precedes successful memory encoding: evidence based on intracranial EEG. J Neurosci 31:5392-5397.

Foster BL, Kaveh A, Dastjerdi M, Miller KJ, Parvizi J (2013) Human retrosplenial cortex displays transient theta phase locking with medial temporal cortex prior to activation during autobiographical memory retrieval. J Neurosci 33:10439-10446.

Fox MD, Halko MA, Eldaief MC, Pascual-Leone A (2012) Measuring and manipulating brain connectivity with resting state functional connectivity magnetic resonance imaging (fcMRI) and transcranial magnetic stimulation (TMS). Neuroimage 62:2232-2243.

Freedberg M, Reeves JA, Toader AC, Hermiller MS, Voss JL, Wassermann EM (2019) Persistent Enhancement of Hippocampal Network Connectivity by Parietal rTMS Is Reproducible. eNeuro 6.

Friedman L, Glover GH (2006) Report on a multicenter fMRI quality assurance protocol. J Magn Reson Imaging 23:827-839.

Goyal A, Miller J, Watrous AJ, Lee SA, Coffey T, Sperling MR, Sharan A, Worrell G, Berry B, Lega B, Jobst BC, Davis KA, Inman C, Sheth SA, Wanda PA, Ezzyat Y, Das SR, Stein J, Gorniak R, Jacobs J (2018) Electrical Stimulation in Hippocampus and Entorhinal Cortex Impairs Spatial and Temporal Memory. J Neurosci 38:4471-4481.

Hanslmayr S, Axmacher N, Inman CS (2019) Modulating Human Memory via Entrainment of Brain Oscillations. Trends Neurosci 42:485-499.

Hebscher M, Voss JL (in press) Testing network properties of episodic memory using non-invasive brain stimulation. Current opinion in behavioral sciences.
Hermiller MS, VanHaerents S, Raij T, Voss JL (2018) Frequency-specific noninvasive modulation of memory retrieval and its relationship with hippocampal network connectivity. Hippocampus.
Hermiller MS, Karp E, Nilakantan AS, Voss JL (2019) Episodic memory improvements due to noninvasive stimulation targeting the cortical-hippocampal network: A replication and extension experiment. Brain Behav 9:e01393.
Herweg NA, Solomon EA, Kahana MJ (2020) Theta Oscillations in Human Memory. Trends Cogn Sci 24:208-227.
Huang YZ, Edwards MJ, Rounis E, Bhatia KP, Rothwell JC (2005) Theta burst stimulation of the human motor cortex. Neuron 45:201-206.
Jacobs J, Miller J, Lee SA, Coffey T, Watrous AJ, Sperling MR, Sharan A, Worrell G, Berry B, Lega B, Jobst BC, Davis K, Gross RE, Sheth SA, Ezzyat Y, Das SR, Stein J, Gorniak R, Kahana MJ, Rizzuto DS (2016) Direct Electrical Stimulation of the Human Entorhinal Region and Hippocampus Impairs Memory. Neuron 92:983-990.
Kim H (2011) Neural activity that predicts subsequent memory and forgetting: a meta-analysis of 74 fMRI studies. Neuroimage 54:2446-2461.
Kim S, Nilakantan AS, Hermiller MS, Palumbo RT, VanHaerents S, Voss JL (2018) Selective and coherent activity increases due to stimulation indicate functional distinctions between episodic memory networks. Sci Adv 4:eaar2768.
Kohler S, Paus T, Buckner RL, Milner B (2004) Effects of left inferior prefrontal stimulation on episodic memory formation: a two-stage fMRI-rTMS study. J Cogn Neurosci 16:178-188.
Kucewicz MT, Berry BM, Miller LR, Khadjevand F, Ezzyat Y, Stein JM, Kremen V, Brinkmann BH, Wanda P, Sperling MR, Gorniak R, Davis KA, Jobst BC, Gross RE, Lega B, Van Gompel J, Stead SM, Rizzuto DS, Kahana MJ, Worrell GA (2018) Evidence for verbal memory enhancement with electrical brain stimulation in the lateral temporal cortex. Brain 141:971-978.
Lisman JE, Jensen O (2013) The theta-gamma neural code. Neuron 77:1002-1016.
Mesulam MM, Van Hoesen GW, Pandya DN, Geschwind N (1977) Limbic and sensory connections of the inferior parietal lobule (area PG) in the rhesus monkey: a study with a new method for horseradish peroxidase histochemistry. Brain Res 136:393-414.
Miller JP, Sweet JA, Bailey CM, Munyon CN, Luders HO, Fastenau PS (2015) Visual-spatial memory may be enhanced with theta burst deep brain stimulation of the fornix: a preliminary investigation with four cases. Brain 138:1833-1842.
Moisa M, Pohmann R, Ewald L, Thielscher A (2009) New coil positioning method for interleaved transcranial magnetic stimulation (TMS)/functional MRI (fMRI) and its validation in a motor cortex study. J Magn Reson Imaging 29:189-197.
Mufson EJ, Pandya DN (1984) Some observations on the course and composition of the cingulum bundle in the rhesus monkey. J Comp Neurol 225:31-43.
Nilakantan AS, Mesulam MM, Weintraub S, Karp EL, VanHaerents S, Voss JL (2019) Network-targeted stimulation engages neurobehavioral hallmarks of age-related memory decline. Neurology 92:e2349-e2354.
Paller KA, Wagner AD (2002) Observing the transformation of experience into memory. Trends Cogn Sci 6:93-102.
Poppenk J, Evensmoen HR, Moscovitch M, Nadel L (2013) Long-axis specialization of the human hippocampus. Trends Cogn Sci 17:230-240.
Ranganath C, Ritchey M (2012) Two cortical systems for memory-guided behaviour. Nat Rev Neurosci 13:713-726.
Ranganath C, Yonelinas AP, Cohen MX, Dy CJ, Tom SM, D'Esposito M (2004) Dissociable correlates of recollection and familiarity within the medial temporal lobes. Neuropsychologia 42:2-13.
Romei V, Thut G, Silvanto J (2016) Information-Based Approaches of Noninvasive Transcranial Brain Stimulation. Trends Neurosci 39:782-795.
Rossi S, Hallett M, Rossini PM, Pascual-Leone A, Group SoTC (2009) Safety, ethical considerations, and application guidelines for the use of transcranial magnetic stimulation in clinical practice and research. Clin Neurophysiol 120.

Rutishauser U, Ross IB, Mamelak AN, Schuman EM (2010) Human memory strength is predicted by theta-frequency phase-locking of single neurons. Nature 464:903-907.
Shirvalkar PR, Rapp PR, Shapiro ML (2010) Bidirectional changes to hippocampal theta-gamma comodulation predict memory for recent spatial episodes. Proc Natl Acad Sci U S A 107:7054-7059.
Siebner HR et al. (2009) Consensus paper: combining transcranial stimulation with neuroimaging. Brain Stimul 2:58-80.
Small SA, Schobel SA, Buxton RB, Witter MP, Barnes CA (2011) A pathophysiological framework of hippocampal dysfunction in ageing and disease. Nat Rev Neurosci 12:585-601.
Squire LR, Zola-Morgan S (1991) The medial temporal lobe memory system. Science 253:1380-1386.
Squire LR, Stark CE, Clark RE (2004) The medial temporal lobe. Annu Rev Neurosci 27:279-306.
Stark CE, Squire LR (2001) When zero is not zero: the problem of ambiguous baseline conditions in fMRI. Proc Natl Acad Sci U S A 98:12760-12766.
Staudigl T, Hanslmayr S (2013) Theta oscillations at encoding mediate the context-dependent nature of human episodic memory. Curr Biol 23:1101-1106.
Stern CE, Corkin S, Gonzalez RG, Guimaraes AR, Baker JR, Jennings PJ, Carr CA, Sugiura RM, Vedantham V, Rosen BR (1996) The hippocampal formation participates in novel picture encoding: evidence from functional magnetic resonance imaging. Proc Natl Acad Sci U S A 93:8660-8665.
Tambini A, Nee DE, D'Esposito M (2018) Hippocampal-targeted Theta-burst Stimulation Enhances Associative Memory Formation. J Cogn Neurosci 30:1452-1472.
Thickbroom GW (2007) Transcranial magnetic stimulation and synaptic plasticity: experimental framework and human models. Exp Brain Res 180:583-593.
Thut G, Schyns PG, Gross J (2011a) Entrainment of perceptually relevant brain oscillations by non-invasive rhythmic stimulation of the human brain. Front Psychol 2:170.
Thut G, Veniero D, Romei V, Miniussi C, Schyns P, Gross J (2011b) Rhythmic TMS causes local entrainment of natural oscillatory signatures. Curr Biol 21:1176-1185.
Thut G, Bergmann TO, Frohlich F, Soekadar SR, Brittain JS, Valero-Cabre A, Sack AT, Miniussi C, Antal A, Siebner HR, Ziemann U, Herrmann CS (2017) Guiding transcranial brain stimulation by EEG/MEG to interact with ongoing brain activity and associated functions: A position paper. Clin Neurophysiol 128:843-857.
Titiz AS, Hill MRH, Mankin EA, Aghajan ZM, Eliashiv D, Tchemodanov N, Maoz U, Stern J, Tran ME, Schuette P, Behnke E, Suthana NA, Fried I (2017) Theta-burst microstimulation in the human entorhinal area improves memory specificity. Elife 6.
Wang JX, Rogers LM, Gross EZ, Ryals AJ, Dokucu ME, Brandstatt KL, Hermiller MS, Voss JL (2014) Targeted enhancement of cortical-hippocampal brain networks and associative memory. Science 345:1054-1057.
Warren K, Hermiller MS, Nilakantan A, Voss JL (2020) Stimulating the hippocampal posterior-medial network enhances task-dependent connectivity and memory. Elife.
Warren KN, Hermiller MS, Nilakantan AS, O'Neil J, Palumbo RT, Voss JL (2018) Increased fMRI activity correlations in autobiographical memory versus resting states. Hum Brain Mapp 39:4312-4321.
Xia M, Wang J, He Y (2013) BrainNet Viewer: a network visualization tool for human brain connectomics. PLoS One 8:e68910.
Xiao JX, Ehinger KA, Hays J, Torralba A, Oliva A (2016) SUN Database: Exploring a Large Collection of Scene Categories. International Journal of Computer Vision 119:3-22.
Yonelinas AP (2001) Consciousness, control, and confidence: the 3 Cs of recognition memory. J Exp Psychol Gen 130:361-379.
Yonelinas AP (2002) The nature of recollection and familiarity: A review of 30 years of research. Journal of Memory and Language 46:441-517.
Zutshi I, Brandon MP, Fu ML, Donegan ML, Leutgeb JK, Leutgeb S (2018) Hippocampal Neural Circuits Respond to Optogenetic Pacing of Theta Frequencies by Generating Accelerated Oscillation Frequencies. Curr Biol 28:1179-1188 e1173.

Table 1. Behavioral performance. For the test phase in both sessions, the total hit rate (i.e., both Remember and Familiar responses) and the proportion of hits that were recollected (i.e., Remember responses; R if hit) are provided for the scenes that were presented during the study phases for the HNT and SMA location conditions, for trials with stimulation (TMS ON) and without (TMS OFF). The total false alarm rate (i.e., both Remember and Familiar responses) and the proportion of false alarms that were endorsed with recollection (R if false alarm) are provided for scenes that were not presented during the study phase (and thus, were only specific to the session). Values reported for the HNT TBS condition of interest are in bold font; control conditions that significantly differ from the HNT TBS condition in two-tailed t-tests are indicated (~ P<0.1, * P<0.05, ** P<0.01). TMS OFF values that significantly differ via two-tailed t-tests from the corresponding TMS ON condition (i.e., value in row directly above) are indicated (~ P<0.1, * P<0.05, ** P<0.01). Across-participant means (SD).

	TBS session		Beta stimulation session	
	HTN	SMA	HTN	SMA
Total hit rate, TMS ON	**0.66 (0.10)**	0.61 (0.16)	0.67 (0.12)	0.66 (0.16)
Total hit rate, TMS OFF	0.63 (0.13)	0.62 (0.19)	0.62 (0.15) *	0.64 (0.13)
Recollection hits, TMS ON	**0.56 (0.13)**	0.42 (0.15) **	0.48 (0.19) ~	0.46 (0.21) ~
Recollection hits, TMS OFF	0.48 (0.18) *	0.47 (0.20)	0.44 (0.21)	0.43 (0.22)
Total false alarm rate	**0.31 (0.17)**		0.38 (0.12) *	
Recollection false alarms	**0.17 (0.10)**		0.21 (0.23)	